Phosphorus behavior in sediments during a sub-seabed CO_2 controlled release experiment

Ayumi Tsukasaki[a]*, Masahiro Suzumura[a], Anna Lichtschlag[b], Henrik Stahl[c, d] and Rachael H. James[e]

[a]*Research Institute for Environmental Management Technology, National Institute of Advanced Industrial Science and Technology (AIST), AIST Tsukuba West, 16-1 Onogawa, Tsukuba, Ibaraki 305-8569, Japan*

[b]*National Oceanography Centre Southampton, University of Southampton Waterfront Campus, European Way, Southampton SO14 3ZH, UK*

[c]*The Scottish Association for Marine Science, Scottish Marine Institute, Oban, Argyll PA37 1QA, UK*

[d]*Zayed University, PO Box 19282, Dubai, United Arab Emirates*

[e]*Ocean and Earth Science, National Oceanography Centre Southampton, University of Southampton Waterfront Campus, European Way, Southampton SO14 3ZH, UK*

*Corresponding author. Tel.: +81-29-861-3789; fax: +81-29-861-8392.

E-mail address: ayumi-tsukasaki@aist.go.jp (Ayumi Tsukasaki)

Highlights

- ✓ Behavior of sedimentary phosphorus (P) during sub-seabed controlled release of CO_2.
- ✓ Potential P release from CO_2 exposure varies widely as a function of sediment type.
- ✓ Calcium-bound P acts as a source for P released by low pH induced by CO_2.
- ✓ Iron-bound P acts as a sink for P released by low pH induced by CO_2.

Abstract

The CO_2 controlled release experiment "Quantifying and Monitoring Potential Ecosystem Impacts of Geological Carbon Storage" (QICS) assessed the impacts of potential CO_2 leakage from sub-seabed carbon capture and storage reservoirs to the marine environment. During QICS, CO_2 gas was released into shallow sediment in Ardmucknish Bay, Scotland, in the spring and summer of 2012. As part of this project, we investigated the effects of CO_2 leakage on sedimentary phosphorus (P), an essential nutrient for marine productivity. We found no statistically significant effects during QICS, as the solid-phase P content in the sediment was constant before, during, and after exposure to CO_2. However, laboratory experiments using marine sediment standard materials as well as QICS sediment revealed substantial differences among these different sediment types in their potential for P release during CO_2 exposure. Employing the SEDEX sequential extraction technique to determine the sizes of the major P pools in the sediments, we showed that calcium-bound P can be easily released by CO_2 exposure, whereas iron-bound P is a major sink of released P. The overall impacts of CO_2 leakage on sediment P behavior appear to be low compared to natural variability.

Keywords:

Sub-seabed carbon capture and storage; CCS; CO_2 leakage; marine sediment; phosphorus; sequential extraction.

1. Introduction

Long-term storage of carbon dioxide (CO_2) beneath the seafloor promises to help mitigate global climate change by reducing anthropogenic CO_2 emissions into the atmosphere (IPCC, 2005). However, one risk associated with this carbon capture and storage (CCS) technology is the potential for CO_2 leakage due to failures of the pipeline infrastructure and injection wells or due to leakage through ruptures in the caprock, which may be created by events such as earthquakes (Monastersky, 2013; Van Noorden, 2010).

The impact of CO_2 leakage on the marine environment is a special concern (De Vries et al., 2013; Widdicombe et al., 2013). To date, most of our information about the effects of elevated atmospheric concentrations of CO_2 on marine ecosystems comes from studies of ocean acidification (Gattuso et al., 2008; Kleypas et al., 2006; Orr et al., 2005; Royal Society, 2005). Some of these have shown that seawater acidification can alter the biogeochemical cycles of nutrients. Huesemann et al. (2002) found that high levels of CO_2 inhibit nitrification in the water column. Indexes of bioavailability of phosphorus (P) for marine microbes can be altered by changes in pH due to increased CO_2. Uptake rates of P by phytoplankton and phosphatase activities increase or decrease depending on the location and community structure (Endres et al., 2013; Yamada and Suzumura, 2010). To examine the impact of high CO_2 levels on benthic biota, in situ CO_2 exposure experiments have been conducted, but these are restricted to brief and localized experiments using benthic chambers (Ishida et al., 2005, 2013).

In the recent experiment "Quantifying and Monitoring Potential Ecosystem Impacts of

65 Geological Carbon Storage" (QICS), 4.2 t of CO_2 gas was released through a pipeline drilled from
66 land into unconsolidated sediments about 11 m below the seabed (Blackford and Kita, 2013;
67 Blackford et al., 2014). The gas was released over a period of 37 days, and the effects were
68 monitored for a further 90 days. As part of the QICS experiment, we investigated the impacts of
69 CO_2 leakage on the behavior of P in the marine sediments.
70 Although P is an essential nutrient for sustaining marine productivity, an excess of P can
71 degrade water quality through eutrophication and the triggering of harmful algal blooms in coastal
72 ecosystems (Conley et al., 2009). Sediment is an important sink in the oceanic P cycle
73 (Benitez-Nelson, 2000; Paytan and McLaughlin, 2007), and sediment plays an essential role in
74 regulating P availability in shallow coastal environments through P release to and uptake from the
75 water column (e.g., Fisher et al., 1982; Slomp et al., 2013). Release and uptake of P by sediments
76 largely depend on the environmental conditions (e.g., redox potential, pH, activities of benthic
77 organisms) and the reactivity of the different geochemical pools of P in the sediment (Mayer and
78 Jarrell, 2000; Ruttenberg, 1992). Through its role as a major factor controlling sediment pH, CO_2
79 can regulate the behavior of P in sediments.
80 Our objective was to evaluate to what extent CO_2 leakage from CCS reservoirs into the
81 overlying sediment and seawater can induce changes in sedimentary P behavior. During the QICS
82 field experiment, we recorded the changes in P concentration in sediments before, during, and after
83 the CO_2 release in both the solid phase and pore water. We also conducted laboratory experiments
84 to evaluate the potential for P release from the sediment solid phase due to CO_2 exposure, using

85 standard reference materials of coastal and pelagic marine sediments as well as a sediment sample
86 collected from the QICS site. We used a sequential extraction technique to identify the pools of P in
87 sediment that are most sensitive to changes in CO_2 levels.
88
89 **2. Materials and methods**
90 **2.1 QICS field experiment and sampling**
91 The CO_2 release experiment was conducted in Ardmucknish Bay, on the west coast of
92 Scotland. A pipeline was drilled from land into shallow sediment 350 m offshore. CO_2 gas was
93 introduced into the sediment through a perforated diffuser (0.5 mm holes) at the end of the pipeline
94 11 m below the seabed. The depth of the overlying water column was 10–12 m, depending on the
95 state of the tide. A total of 4.2 t of CO_2 gas was injected over 37 days between 17 May and 22 June
96 2012, and the site was monitored for a further 90 days. CO_2 was initially injected at a rate of 10
97 kg/d, and then the injection rate was incrementally increased to 210 kg/d. Full details of the
98 experimental setup are given elsewhere (Blackford et al., 2014; Taylor et al., this issue).
99 Core samples of sediment were collected from directly above the CO_2 injection site (QICS
100 Zone 1; Z1) during six campaigns: (1) 10 May, seven days prior to the start of CO_2 release (D –7),
101 (2) 30–31 May (D 13/14, during injection), (3) 20–21 June (D 34/35, during injection), (4) 28–29
102 June (D 42/43, 5–6 days after the end of injection), (5) 9–10 July (D 54/55, 17–18 days after the
103 injection), and (6) 20–21 September (D 126/127, 89–90 days after the injection). Another core
104 sample was collected within an active pockmark close to a bubble stream (Zone 1 pockmark; Z1*p*)

105 on D 34/35. Cores were collected by SCUBA divers using acrylic tubes (5 cm i.d.). Immediately
106 after collection, pore water in the cores was extracted by filtering with Rhizon Pore Water
107 Samplers (pore size 0.15 μm, Rhizosphere Research Products, Netherlands). Subsamples of the
108 filtered pore water were fixed with mercuric chloride for dissolved inorganic carbon (DIC) analysis
109 or frozen for dissolved inorganic phosphorus (DIP) analysis. The sediment cores were sliced into
110 sections 2 cm thick in a temperature-controlled room set at in situ temperature (~8 °C), freeze-dried,
111 and then homogenized with an agate mortar and pestle (details in Lichtschlag et al., this issue).
112
113 **2.2 Laboratory CO_2 exposure experiment**
114 To quantify the potential for P release from different types of sediment, we conducted a series
115 of laboratory CO_2 exposure experiments using standard reference materials and a sediment sample
116 from the QICS site. Reference materials representing coastal and pelagic marine sediments (JMS-1
117 and JMS-2, respectively) were provided by the Geological Survey of Japan. The JMS-1 sediment
118 was collected from a eutrophic coastal basin (Tokyo Bay), and the JMS-2 sediment was a mixture
119 of pelagic and zeolitic clay from seven locations in the South Pacific (Terashima et al., 2002). The
120 QICS sample consisted of sediment from 0–2 cm depth, collected from site Z1 prior to release of
121 CO_2.
122 A schematic diagram of the experiment is shown in Figure 1. A 0.30 g sediment sample was
123 placed into a polycarbonate centrifuge tube and 30 mL of P-depleted pelagic seawater collected
124 from the surface of the western North Pacific Ocean (155°E, 20°N) was added. The concentration

of DIP, as a measure of dissolved orthophosphate, in the seawater sample was below detection limit (< 0.02 μM). The seawater was filtered through a 0.2 μm Nuclepore filter (Whatman, UK) before use to minimize microbiological influences, then saturated with CO_2 by bubbling just before the experiment. The mixture of sediment and seawater was continuously bubbled with CO_2 gas for 24 hours at 25 °C. To evaluate the effects of physical disturbance by bubbling, parallel experiments bubbling laboratory air (rather than CO_2) were conducted as a control. After 24 hours, the mixture was centrifuged (4000 rpm, 2380 *g* for 10 min), and the supernatant was analyzed for DIP. Another 30 mL aliquot of filtered seawater was then added to the same sediment sample, and this procedure was repeated five times such that six sequential experiments were run for each sediment type.

2.3 Chemical analysis

The total P content of the sediment solid phase (total P) was determined in the freeze-dried samples by using the method of Aspila et al. (1976), slightly modified by Suzumura (2008). Briefly, 0.5 mL of 0.17 M magnesium nitrate was added to 0.1 g of sediment, and then the mixture was dried on a hotplate and combusted at 470 °C for 90 min. DIP was extracted with 1 M hydrochloric acid and determined spectrophotometrically with a Seal Analytical QuAAtro Autoanalyser (2-HR, UK). To determine DIP concentrations of the pore water samples, the frozen samples were thawed, diluted 20 times, and then measured with the Autoanalyser. DIC in the pore water samples was measured by using an Apollo SciTech DIC analyzer (AS-C3) with a CO_2/H_2O infrared analyzer (LI-7000, LI-COR, USA) to detect CO_2 released from the sample after acidifying with 10%

145 H_3PO_4.

146 The different geochemical reservoirs of P were quantified by using a sequential extraction
147 technique (SEDEX) following Ruttenberg (1992). Approximately 0.30 g of sediment (both the
148 original sediment and the sediment subjected to bubbling with CO_2 or air) was extracted
149 sequentially with 30 mL of (1) 1 M magnesium chloride (pH 8), (2) citrate dithionite buffer (CDB;
150 pH 7.6), (3) 1 M sodium acetate buffer (pH 4), and (4) 1 M hydrochloric acid. In step 5, the residue
151 from step 4 was ashed at 550 °C and extracted with 30 mL of 1 M hydrochloric acid. After
152 extraction steps 1, 2 and 3, sediment samples were rinsed first with 1 M magnesium chloride (30
153 mL), then with water (30 mL) to prevent the readsorption of extracted phosphate. The extraction
154 and washing solutions were centrifuged (4000 rpm, 2380 *g* for 10 min) and filtered through a
155 syringe filter with 0.45 μm pore size (Millex-HV, Millipore, USA). The supernatants containing
156 magnesium chloride or sodium acetate buffer were acidified to pH 1 by the addition of
157 hydrochloric acid, and DIP analysis followed. The CDB extracts are not suited to analysis by the
158 standard molybdenum blue method because the citrate interferes with reduction of molybdate
159 complex (Ruttenberg, 1992); therefore, a solid-phase extraction technique was used (Suzumura
160 and Koike, 1995). All reagents used were of analytical grade. Purified water obtained from a
161 Milli-Q Gradient System (Millipore, USA) was used for reagent preparation and rinse. Three
162 replicate measurements were carried out for total P analysis and SEDEX. All results of this
163 procedure are reported on an oven-dry (110 °C) basis.

164 The chemical composition of the sediments was determined by energy-dispersive X-ray

fluorescence spectrometry (EDXL300, Rigaku, Japan). Loss-on-ignition (LOI) was determined after heating for 1 hour at 750 °C (JIS, 2009). The carbonate content of the sediments was determined by using a CO_2 coulometer (Coulometrics, USA) that measures the CO_2 released during sample dissolution under acidic conditions (10% phosphoric acid) in a closed system (Johnson et al., 1987). The Brunauer-Emmett-Teller (BET) specific surface area of the sediments was determined by nitrogen adsorption (BELSORP-max, BEL JAPAN, Japan).

2.4 Calculations and statistical analysis

Results are reported as the mean ± 1 standard deviation (SD), where applicable. For statistical analyses, we used the program SigmaStat, included in the Sigmaplot 11 software package (Systat Software, Chicago, USA). We used a significance level of 5%.

3. Results and discussion

3.1 Total P concentration in QICS sediment from the field experiment

Vertical profiles of total P in the QICS sediment are shown in Figure 2. Total P concentrations at site Z1 before CO_2 injection were ~14 μmol/g (12.6–14.2 μmol/g; Fig. 2a) and showed little variation with depth. The total P concentrations that we measured in the Ardmucknish Bay sediments were somewhat lower than values reported for other continental margins and coastal areas (~34 μmol/g; e.g., Frankowski et al., 2002; Küster-Heins et al., 2010; Suzumura, 2008). During and after exposure to CO_2, we observed no obvious changes in total P (Fig. 2). Although

concentrations of DIC in the sediment pore water increased significantly below 20 cm depth 35 days after the start of the CO_2 release (Blackford et al., 2014; Lichtschlag et al., this volume), total P concentrations (11.8–16.6 µmol/g; Fig. 2b) were close to those observed before the CO_2 release (12.6–14.2 µmol/g). The highest levels of pore-water DIC (10 times background levels) were observed for five days after the release of CO_2 was terminated, but there was no obvious effect on total P concentration during this period (12.5–15.6 µmol/g; Fig. 2c). Throughout the experiment, changes in the total P content of the sediments were not statistically significant (ANOVA; $p = 0.126$, $n = 8$). Figure 2d shows the vertical profile of total P at the bubble stream site (Z1*p*) after the start of the CO_2 injection (D 34/35). Again, changes in the total P content of these sediments, relative to the other sediment cores collected from Z1, were not significant (paired *t*-test, $p = 0.803$, $n = 12$). These results indicate that leakage of CO_2 had no effect on the total P content of Ardmucknish Bay sediments. DIP concentrations in sediment pore water varied vertically, ranging between ~3 and ~7 µmol/L, before the CO_2 release (Fig. 3a). DIP in pore water increased slightly with high DIC concentrations at D 34/35 at site Z1 (up to 13 µmol/L; Fig. 3b), but this increase was not observed in pore water with high DIC from site Z1*p* (Fig. 3d). These fluctuations in DIP concentration observed during the QICS field experiment are unexplained.

3.2 Laboratory CO_2 exposure experiment

To assess whether the lack of any obvious change in the total P content of the Ardmucknish Bay sediments during the QICS experiment was due to non-reactive forms of P in these sediments,

205 or the rate and amount of CO_2 released, a series of laboratory experiments were performed. In our
206 laboratory experiments, sediment samples were exposed to high levels of CO_2 (equivalent to
207 approximately 30 mmol/L as DIC) to assess the role of non-reactive P. The concentration of DIP in
208 seawater increased when either CO_2 or air was bubbled through the sediment suspension. The
209 amount of DIP released from the sediment solid phase ($P_{released}$), as estimated from the measured
210 DIP concentration of seawater, decreased gradually over the course of the experiment, but DIP was
211 still being released even after five episodes of bubbling (Fig. 4a). To estimate the potential
212 maximum amount of releasable P in the sediment solid phase, we assumed that the P concentration
213 was in solid-liquid equilibrium and fitted the following equation to our data:

214 $$\Sigma P_{released} = (1 - q^n) P_{max},$$

215 where P_{max} is the maximum amount of releasable P (μmol P/g) as obtained by extending each
216 regression curve in Figure 4a to infinity, n is the number of bubbling episodes, and q is the
217 fractionation coefficient, defined as releasable P content remaining in the sediment per DIP content
218 in seawater plus releasable P content remaining in the sediment. The fit is good between our data
219 and this equation ($r^2 > 0.96$, $p < 0.01$, $n = 6$). The calculated values of P_{max} from the CO_2 bubbling
220 experiment (CO_2-P_{max}) for QICS sediment from site Z1 was 0.83 ± 0.11 μmol/g ($n = 6$). This value
221 is equivalent to 6.0% of the total P in the sediment (Table 1). Such small changes in total P would
222 be difficult to detect in the QICS field experiment, even in sediments exposed to very high levels of
223 CO_2. With one outlier, P_{max} induced by air bubbling (Air-P_{max}) in the QICS sediment was 0.69 ±
224 0.01 μmol/g ($n = 5$), accounting for 4.9% of total P. The difference between CO_2-P_{max} and Air-P_{max}

225 corresponds to the potential amount of releasable P due to leakage of CO_2. Although the difference
226 between CO_2-P_{max} and Air-P_{max} was significant ($p < 0.05$), the amount of the difference, 0.14
227 μmol/g, is equivalent to only 1.0% of total P. This result implies that most of the P released by
228 bubbling is due to physical disturbance of the sediments, and leakage of CO_2 does not lead to
229 notable change in the total P content of sediments in Ardmucknish Bay. The stability of total P
230 concentrations during the QICS field experiment is therefore most likely because the sediment P
231 was in forms that were not reactive to CO_2 exposure.
232 To assess whether the non-reactivity of P with respect to CO_2 is a general property of marine
233 sediments or is specific to the sediments in Ardmucknish Bay, we performed laboratory
234 experiments using two standard reference marine sediments (JMS-1 and JMS-2). The results are
235 shown in Figures 4b and c and in Table 1. The rate and extent of P release differed substantially
236 between the different sediment samples. For the coastal marine sediment (JMS-1), the release of P
237 in the air bubbling experiment (Air-P_{max}; 1.27 ± 0.30 μmol/g) was nearly twice that in the CO_2
238 bubbling experiment (CO_2-P_{max}; 0.66 ± 0.12 μmol/g). These results suggest that although the
239 physical disturbance of bubbling induced P release from the JMS-1 sediment regardless of gas type,
240 P release was considerably depressed by exposure to CO_2. In the pelagic marine sediment (JMS-2),
241 P release was greatly enhanced by CO_2 bubbling, such that CO_2-P_{max} (13.84 ± 3.31 μmol/g) was an
242 order of magnitude higher than for the other sediments (Table 1). On the other hand, Air-P_{max} of the
243 JMS-2 sediment was comparable to its value in the QICS and JMS-1 sediments. In addition, the
244 proportion of P release induced by CO_2 (CO_2-P_{max} - Air-P_{max}) to total P was substantially higher in

245 the JMS-2 sediment (7.3%). The considerable difference in P dissolution behavior among the three
246 different sediment types is most likely due to differences in the P pools and their reactivity with
247 CO_2.

248 During the laboratory experiment, pH values were generally constant (8.07 ± 0.06, n = 90)
249 among three sediments throughout all five episodes of air bubbling, but they varied greatly with
250 CO_2 bubbling (Fig. 5). The CO_2 bubbling experiments produced the highest pH values in seawater
251 during the first bubbling episode for all sediment samples, particularly in JMS-2 (5.40 ± 0.05, n =
252 6). This value was significantly higher ($p < 0.01$) than the pH range in the QICS sediment (5.17 ±
253 0.04, n = 6) and JMS-1 (5.19 ± 0.03, n = 6). The pH decreased to a constant value of ~5.0 after the
254 second bubbling episode in the QICS and JMS-1sediments. However, pH in the JMS-2 sediment
255 decreased more gradually, reaching 5.12 ± 0.02 (n = 6) after the second bubbling episode and
256 stabilizing at ~5.0 after the third bubbling episode. The higher pH in the initial stages was likely due
257 to buffering by carbonates in the sediments. This would imply that JMS-2 had the highest buffering
258 capacity of the three sediments, which might be related to the greater P release from JMS-2 than
259 from QICS and JMS-1 after CO_2 exposure. To confirm this, further chemical analyses were
260 performed.

261

262 **3.3 Chemical forms of P in sediments**

263 For a better understanding of P behavior during CO_2 exposure, we quantified the various forms
264 of P in the sediments, both before and after bubbling, using the well-established SEDEX method

(Ruttenberg, 1992). In SEDEX, the strength of the extractant is incrementally increased to separate more strongly bound P. The P fractions extracted by the first three steps—loosely sorbed P (step 1), iron-bound P (step 2), and calcium-bound P (step 3)—are considered to be easily releasable, for example, by changes in environmental conditions. Step 4 extracts detrital P, and step 5 extracts organic P (Fig. 6).

There were substantial differences in P composition among the sediments before bubbling (original sediments). The original QICS sediment was dominantly detrital P, which accounted for 71% of the total extracted P from all five steps. Original sediment JMS-1 contained large proportions of organic P (28%) and iron-bound P (31%). Original sediment JMS-2 was dominantly calcium-bound P (30%) and detrital P (48%). These results are consistent with the bulk chemical analyses, which showed that JMS-2 had the highest contents of calcium and carbonates (Tables 2 and 3).

Although CO_2 and air bubbling released P (as DIP) from the QICS sediment into seawater (Table 1), the difference between P extracted by SEDEX from the original sediment (14.7 ± 0.78 μmol/g) and the bubbled sediment (air: 14.1 ± 0.31 μmol/g, CO_2: 14.3 ± 0.54 μmol/g) was not significant (*t*-test, $p > 0.05$, $n = 3$). Two factors likely account for the lack of significance: first, the accumulated error over the steps of the SEDEX procedure is large compared to the difference between the original and bubbled sediments. Second, the concentration difference between the solid phase (μmol/g) and solution phases (μmol/L) is necessarily very large, such that small changes in the solid phase that are less than the limits of detection can cause detectable changes in

285 the solution phase.

286 In the JMS-1 sediment, the total P extracted by SEDEX from the original, air-bubbled, and
287 CO_2-bubbled samples was 20.8 ± 0.04, 20.2 ± 0.11, and 20.7 ± 0.18 μmol/g, respectively. The
288 decrease in P relative to the original sample in the air-bubbled sample was significant (*t*-test, $p <$
289 0.05, $n = 3$), but it was not significant in the CO_2-bubbled sample (*t*-test, $p > 0.05$, $n = 3$). Although
290 the decrease caused by air bubbling was statistically significant, its magnitude (0.6 μmol/g) was
291 comparable to the decrease in the QICS sediment. CO_2 bubbling increased the content of
292 iron-bound P in JMS-1 significantly relative to the original and the air-bubbled sediments (Fig. 6b).
293 This accounts for the result that P release from the JMS-1 sediment was depressed by CO_2
294 bubbling (Fig. 4b). It appears that the released DIP was redistributed to the iron-bound P pool in
295 this sediment in the amount of 1.43 ± 0.40 μmol/g.

296 In the JMS-2 sediment, much greater changes were observed after CO_2 bubbling: detrital and
297 calcium-bound P decreased, and iron-bound and loosely sorbed P increased by statistically
298 significant amounts ($n = 3$, $p < 0.01$). According to Ruttenberg (1992), the calcium-bound P
299 fraction contains authigenic apatite, biogenic hydroxyapatite, and calcium carbonate–bound P (e.g.,
300 calcite). Detrital P contains relatively stable inorganic materials, including lithic clasts and minerals
301 such as detrital apatite of igneous or metamorphic origin. It may be that dissolution of abundant
302 apatite species in JMS-2 raised the seawater DIP concentration during the CO_2 bubbling
303 experiment. Redistribution of released P appeared to be greater in JMS-2 than in the JMS-1
304 sediment. It is noteworthy that JMS-2 has the largest specific surface area of the three sediments

305 (Table 3), and therefore the largest number of adsorption sites, as well as the highest iron content
306 (Table 2). The significant increase in loosely sorbed and iron-bound P in JMS-2 after CO_2 bubbling
307 may indicate that some of the DIP released from apatite was subsequently taken up into these pools
308 by adsorption and scavenging. Anderson and Delaney (2000) reported that most loosely sorbed P is
309 composed of phosphate adsorbed on oxides, including iron oxide. Therefore, the increase in
310 loosely sorbed P in JMS-2 after CO_2 bubbling may be P adsorbed on iron oxides, that is,
311 iron-bound P.
312 The behavior and status of calcium-bound and iron-bound P have been studied in solutions
313 over a wide range of pH, regardless of CO_2 concentration. It has been shown that DIP is released
314 from calcium-bound P and incorporated into iron-bound P at pH 6.0 or lower (Golterman, 1995;
315 Gomez et al., 1999). The substantial changes in the P pools in the JMS-2 sediment, therefore, were
316 most likely induced by changes in pH during CO_2 bubbling. Consistent with that finding, we
317 observed a small but significant increase in iron-bound P in the JMS-1 sediment as a result of CO_2
318 bubbling. Iron-bound P may therefore act as a buffer and sink of P released from apatite and other
319 fractions. This effect is likely to be notable under oxic conditions, where iron-bound P is stable (e.g.,
320 Rozan et al., 2002).
321
322 **4. Summary and wider implications**
323 Our experiments found no significant impacts of CO_2 leakage on P behavior in the sediments
324 of Ardmucknish Bay. The laboratory experiments showed that the P content in Ardmucknish Bay

sediments is rather insensitive to CO_2 exposure. Crucially, the QICS sediment has the highest concentration of silica (Table 2) and contains dominantly detrital P (Fig. 6a). Thus, it may be rich in non-apatite detrital materials, which tend to be relatively inert. Our results show that loosely sorbed P and iron-bound P, which are relatively easily mobilized in marine environments, are largely unaffected by CO_2 exposure. On the other hand, CO_2 exposure appears to increase acidic dissolution of calcium carbonates and apatite, which liberates their P content. Although dissolution of calcium carbonate was important in buffering pH changes during the QICS experiment (Blackford et al., 2014), no considerable change in P concentrations of solid phases or pore water was observed during the field experiment. This is likely because calcium-bound P is a minor P pool in the QICS sediment. Moreover, most of the calcium-bound P fraction in the QICS sediment appears to be apatite, which is orders of magnitude less sensitive to acidic dissolution than calcite (Amankonah et al., 1985; Ruben and Bennett, 1987). Our data also show that much of the P released from these phases was redistributed within the other sediment P pools, so the total P content of marine sediments is not an effective indicator of CO_2 leakage in marine environments.

Our results provide insight into the processes that might occur if leaked CO_2 were to reach shallow unconsolidated sediments from deep geological storage (or shallow pipelines). Because P is an essential nutrient, releases of P from sediment to seawater may affect coastal ecosystems. Concentrations of iron-bound P can fluctuate considerably and seasonally in coastal sediments, and such fluctuation might influence the P status of the overlying water column (Slomp et al., 2013; Sundby et al., 1992). Our data show that CO_2 exposure does not result in large P releases in

345 Ardmucknish Bay sediments. Moreover, iron-bound P functions as a sink for P, rather than a source.
346 Although we tested only three sediment samples from different locations, the wide variation in P
347 behavior after CO_2 exposure among these samples emphasizes the importance of proper site
348 assessment at each CCS site. The effects of CO_2 leakage on release of P are negligible relative to
349 the effects of seasonal changes in the redox conditions of coastal marine sediments. This strongly
350 suggests that proper monitoring of baseline conditions is essential to assess the potential impacts of
351 CO_2 leakage on the dynamics of sedimentary phosphorus.
352
353 **Acknowledgments**
354 We thank all of the QICS participants for valuable technical support and scientific exchange, in
355 particular Peter Taylor, Belinda Alker, and Carolyn Graves for support during sampling. We also
356 thank the skilled divers of the National Scientific Diving Facility at the Scottish Association for
357 Marine Science for collecting the cores, as well as the landowners (Lochnell Estate) and users
358 (Tralee Bay Holiday Park) for allowing us to conduct this experiment. Funding was kindly
359 provided by the Natural Environment Research Council (NE/H013962/1), the Scottish
360 Government, and the Ministry of Economy, Trade and Industry of Japan.
361
362

363 ***References***

364

365 Amankonah, J. O., Somasundaran, P., Ananthapadmabhan, K.P. 1985. Effects of dissolved mineral
366 species on the dissolution/precipitation characteristics of calcite and apatite. Colloids and
367 Surfaces 15, 295-307.
368 Anderson, L. D., Delaney, M. L., 2000. Sequential extraction and analysis of phosphorus in marine
369 sediments: Streamlining of the SEDEX procedure. Limnol. Oceanogr. 45, 509-515.
370 Aspila, K. I., Agemian, H., Chau, A. S. Y., 1976. A semi-automated method for the determination
371 of inorganic, organic and total phosphate in sediments. Analyst 101, 187-197.
372 Blackford, J.C., Kita, 2013. A novel experimental release of CO_2 in the marine environment to aid
373 monitoring and impact assessment. Energy Procedia 37, 3387 – 3393.
374 Blackford, J., Stahl, H., Bull, J.M., Bergès, B.J.P., Cevatoglu, M., Lichtschlag, A., Connelly, D.,
375 James, R.H., Kita, J., Long, D., Naylor, M., Shitashima, K., Smith, D., Taylor P., Wright, I.,
376 Akhurst, M., Chen, B., Gernon, T.M., Hauton, C., Hayashi, M., Kaieda, H., Leighton, T.G.,
377 Sato, T., Sayer, M.D.J., Suzumura, M., Tait, K., Vardy, M.E., White P.R., Widdicombe, S., 2014.
378 Detection and impacts of leakage from sub-seafloor deep geological carbon dioxide storage.
379 Nature Climate Change 4, 1011-1016, doi: 10.1038/nclimate2381.
380 Benitez-Nelson, C. R., 2000. The biogeochemical cycling of phosphorus in marine systems. Earth
381 Sci. Rev. 51, 109-135.
382 Conley, D. J., Björck, S., Bonsdorff, E., Carstensen J., Destouni, G., Gustafsson, B. G., Hietanen, S.,
383 Kortekaas, M., Kuosa, H., Meier, H. E. M., Müller-Karulis, B., Nordberg, K., Norkko, A.,
384 Nürnberg, G., Pitkänen, H., Rabalais, N. N., Rosenberg, R., Savchuk, O. P., Slomp, C. P., Voss,
385 M., Wulff, F., Zillen, L., 2009. Hypoxia-related processes in the Baltic Sea. Environ. Sci.
386 Technol. 43, 3412-3420.
387 De Vries, P., Tamis, J.E., Foekema, E.M., Klok, C., Murk, A.J., 2013. Towards quantitative
388 ecological risk assessment of elevated carbon dioxide levels in the marine environment. Mar.
389 Pollut. Bull. 73, 516-523.
390 Endres, S., Unger, J., Wannicke, N., Nausch, M., Voss, M., Engel, A., 2013. Response of *Nodularia*
391 *spumigena* to pCO2 – Part 2: Exudation and extracellular enzyme activities, Biogeosci. 10,
392 567–582, doi:10.5194/bg-10-567-2013, 2013
393 Fisher, T. R., Carson, P. R., Barber, R. T., 1982. Sediment nutrient regeneration in three North

394 Carolina estuaries. Estuarine Coastal Shelf Sci. 14, 101-116.
395 Frankowski, L., Bolałek, J., Szostek, A., 2002. Phosphorus in bottom sediments of Pomeranian
396 Bay (Southern Baltic—Poland). Estuarine Coastal Shelf Sci. 54, 1027-1038.
397 Gattuso, J.-P., Orr, J., Pantoja, S., Pörtner, H.-O., Riebesell, U., Trull, T. (Eds.), 2008. Special Issue:
398 The ocean in the high-CO_2 world II. Biogeosci.
399 http://www.biogeosciences.net/special_issue44.html.
400 Golterman, H. L., 1995. The labyrinth of nutrient cycles and buffers in wetlands; results based on
401 research in the Camargue (Southern France). Hydrobiology 315, 39-58.
402 Gomez, E., Durillon, C., Roffs, G., Picot, B., 1999. Phosphate adsorption and release from
403 sediments of Brackish Lagoons: pH, O_2 and loading influence. Wat. Res. 33, 2437-2447.
404 Huesemann, M.H., A.D. Skillman and E.A. Crecelius, 2002. The inhibition of marine nitrification
405 by ocean disposal of carbon dioxide. Mar. Pollut. Bull. 44, 142-148.
406 IPCC, 2005, IPCC Special Report on Carbon Dioxide Capture and Storage. Prepared by Working
407 Group III of the Intergovernmental Panel on Climate Change [Metz, B., Davidson, O., de
408 Coninck, H. C., Loos, M., Meyer, L. A. (eds.)]. Cambridge University Press, Cambridge,
409 United Kingdom and New York, NY, USA, 442 pp.
410 Ishida, H., Watanabe, Y., Fukuhara, T., Kaneko, S., Furusawa, K., Shirayama, Y., 2005. In situ
411 enclosure experiment using benthic chamber system to assess the effect of high concentration of
412 CO_2 on deep-sea benthic communities. J. Oceanogr. 61, 835–843.
413 Ishida, H., Golmen, L.G., West, J., Krüger, M., Coombs, M., Berge, J. A., Fukuhara, T., Magi, M.,
414 Kita, J., 2013. Effects of CO_2 on benthic biota: An in situ benthic chamber experiment in
415 Storfjorden (Norway). Mar. Pollut. Bull. 73, 443-451.
416 JIS A 1226:2009. Test method for ignition loss of soils.
417 Johnson, K. M., Sieburth, J. McN., Williams, P. J. leB., Brändström, L., 1987. Coulometric total
418 carbon dioxide analysis for marine studies: Automation and calibration. Mar. Chem. 21,
419 117-133.
420 Kleypas, J.A., Feely, R.A., Fabry, V.J., Langdon, C., Sabine, C.L., Robbins, L.L., 2006. Impacts of
421 ocean acidification on coral reefs and other marine calcifiers: a guide for future research, In:
422 Report of a Workshop held 18–20 April 2005, St. Petersburg, FL, sponsored by NSF, NOAA,
423 and the U.S. Geological Survey.
424 Küster-Heins, K., Steinmetz, E., De Lange, G. J., Zabel, M., 2010. Phosphorus cycling in marine
425 sediments from the continental margin off Namibia. Mar. Geol. 274, 95-106.

Lichtschlag, A., James, R. H., Stahl, H., Connely, D., Effect of a controlled sub-seabed release of CO_2 on the biogeochemistry of shallow marine sediments, their pore waters, and the overlying water column. Int. J. Greenhouse Gas Control (2014) this issue.

Mayer, T. D., Jarrell, W. M., 2000. Phosphorus sorption during iron (II) oxidation in the presence of dissolved silica. Wat. Res. 34, 3949-3956.

Monastersky, R., 2013. Seabed scars raise questions over carbon-storage plan. Nature 504, 339–340.

Orr, J.C., Pantoja, S., Pörtner, H.-O., 2005. Introduction to special section: the ocean in a high- CO_2 world. J. Geophys. Res.-Oceans 110, p. C09S01

Paytan, A., McLaughlin, K., 2007. The oceanic phosphorus cycle. Chem. Rev. 107, 563-576.DOI: 10.1021/cr0503613

Royal Society, 2005. Ocean acidification due to increasing atmospheric carbon dioxide. Policy Document 12/05, The Royal Society, London.

Rozan, T. F., Taillefert, M., Trouwborst, R. E., Glazer, B. T., Ma, S., Herszage, J., Valdes, L. M., Price, K. S., Luther III, G. W., 2002. Iron–sulfur–phosphorus cycling in the sediments of a shallow coastal bay: Implications for sediment nutrient release and benthic macroalgal blooms. Limnol. Oceanogr. 47, 1346-1354.

Ruben, J. A., Bennett, A. A., 1987. The evolution of bone. Evolution 41, 1187-1197.

Ruttenberg, K. C., 1992. Development of a sequential extraction method for different forms of phosphorus in marine sediments. Limnol. Oceanogr. 37, 1460-1482.

Slomp, C. P., Mort, H. P., Jilbert, T., Reed, D. C., Gustafsson, B. G., 2013. Coupled dynamics of iron and phosphorus in sediments of an oligotrophic coastal basin and the impact of anaerobic oxidation of methane. PLOS ONE 8, 1-13.

Sundby, B. L., Gobeli, C., Silverberg, N., Mucci, A., 1992. The phosphorus cycle in coastal marine sediments. Limnol. Oceanogr. 37, 1129-1145.

Suzumura, M., 2008. Persulfate chemical wet oxidation method for the determination of particulate phosphorus in comparison with a high-temperature dry combustion method. Limnol. Oceanogr. Methods 6, 619-629.

Suzumura, M., Koike, I., 1995. Application of solid-phase extraction technique for determination phosphorus in sediment extract. Geochem. J. 29, 331-335.Taylor, P., Stahl, H., Vardy, M.E., Bull, J.M., Akhurst, M., Hauton, C., James, R. H., Lichtschlag, A., Long, D., Aleynik, D., Toberman M., Naylor, M., Connelly, D., Smith, D., Sayer, M. D. J., Widdicombe, S., Wright, I.

458 C., Blackford, J., A novel sub-seabed CO_2 release experiment informing monitoring and impact
459 assessment for geological carbon storage. Int. J. Greenhouse Gas Control (2014) this issue.
460 Terashima, S., Imai, N., Taniguchi, M., Okai, T., Nishimura, A., 2002. The preparation and
461 preliminary characterisation of four new geological survey of Japan Geochemical Reference
462 Materials: soils, JSO-1 and JSO-2; and marine sediments, JMS-1 and JMS-2. Geostandards
463 Newslett. 26, 85-94.
464 Van Noorden, R, 2010. Carbon sequestration: Buried trouble Nature 463, 871-873.
465 Widdicombe, S., Blackford, J. C., Spicer, J. I., 2013. Assessing the environmental consequences of
466 CO_2 leakage from geological CCS: Generating evidence to support environmental risk
467 assessment. Mar. Pollut. Bull. 73, 399-401.
468 Yamada, N., Suzumura, M., 2010. Effects of seawater acidification on hydrolytic enzyme activities.
469 J. Oceanogr. 66, 233-241.
470
471
472

Figure captions

Figure 1. Schematic diagram of the CO_2/air exposure experiment.

Figure 2. Vertical profiles of the total P content of sediments collected during the QICS field experiment. (a) Core collected at site Z1 seven days prior to the release of CO_2. (b) Cores collected from site Z1 on days 13/14 and 34/35, during CO_2 release. (c) Cores collected from site Z1 on days 42/43, 54/55, and 126/127 during the recovery phase. (d) Core collected from an active bubble stream, site Z1*p*, on days 34/35. Total P content is on an oven-dry (110 °C) basis.

Figure 3. Vertical profiles of the dissolved inorganic phosphorus (DIP) concentration in sediment pore water collected during the QICS field experiment.

Figure 4. Plots of the integrated amount of P released by bubbling of CO_2 (red) or air (blue) through three sediments: (a) QICS (Z1), (b) JMS-1, and (c) JMS-2. Each sample was bubbled for five separate 24-hour periods. Note difference in scale in 3c relative to 3a and 3b.

Figure 5. Plots of pH during bubbling of CO_2 through QICS sediment (triangles), JMS-1 sediment (open circles), and JMS-2 sediment (filled circles). Each sample was bubbled for five separate periods of 24 hours.

493 Figure 6. P concentration in five different sedimentary P pools before (original) and after bubbling

494 with CO_2 or air for (a) QICS sediment, (b) JMS-1 sediment, and (c) JMS-2 sediment. P content is

495 on an oven-dry (110 °C) basis.

Table1

Table 1. Total P content and maximum amount of releasable P (P_{max}, see text) of sediment samples in the laboratory experiments.

Sample		Mean ± SD (μmol/g)	Proportion of total P (%)
QICS	Total P	13.94 ± 0.14	
	CO_2 P_{max}	0.83 ± 0.11	6.0
	Air P_{max}	0.69 ± 0.01	4.9
JMS-1	Total P	21.52 ± 0.18	
	CO_2 P_{max}	0.66 ± 0.12	3.1
	Air P_{max}	1.27 ± 0.30	5.9
JMS-2	Total P	163.6 ± 0.1	
	CO_2 P_{max}	13.84 ± 3.31	8.5
	Air P_{max}	2.00 ± 0.33	1.2

SD: standard deviation (n = 3 for total P, n = 6 for P_{max}).

Table 2. Major element composition and loss on ignition (LOI) (wt%) of the three sediments in the laboratory experiments.

	Z1	JMS-1	JMS-2
SiO_2	65.50	56.70	46.10
Al_2O_3	11.60	14.50	10.70
Fe_2O_3	0.93	6.14	10.90
CaO	2.15	1.93	4.83
Na_2O	7.41	3.02	4.37
K_2O	2.54	2.17	2.74
MgO	1.36	2.64	4.01
TiO_2	0.31	0.64	1.45
MnO	0.03	0.10	2.37
S	0.46	1.14	0.30
Cl	5.19	2.25	3.49
LOI	2.36	8.71	7.67

Table 3. Carbonate content and specific surface area of the three sediments in the laboratory experiments.

	Z1	JMS-1	JMS-2
Carbonates (mg C/g)	0.90	0.51	1.41
Specific surface area (m^2/g)	1.6	23.7	85.9

Figure 1 (on the web only)

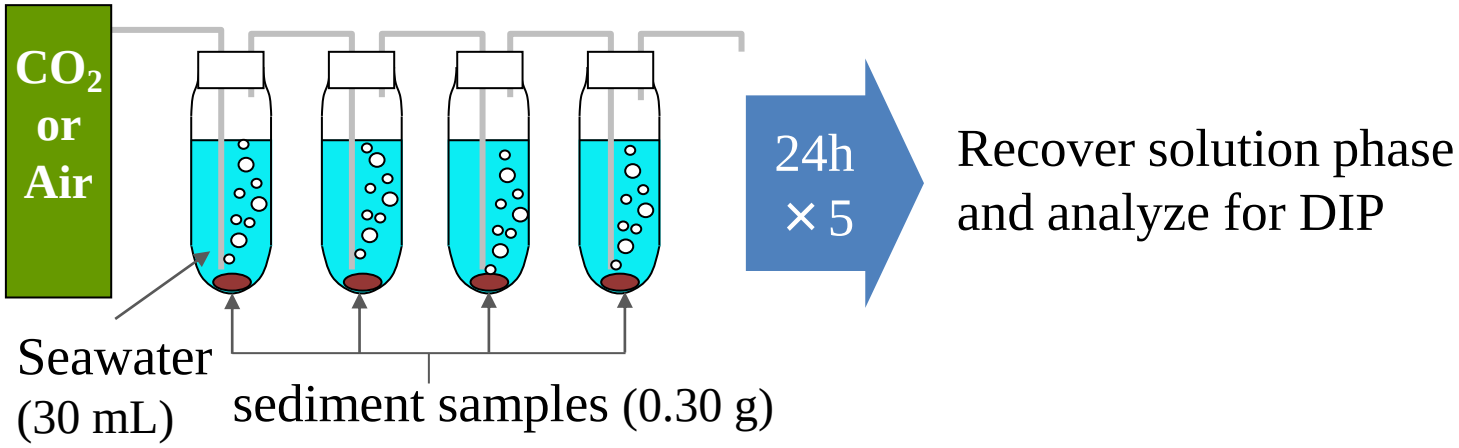

Figure2

Figure 2 (on the web only)

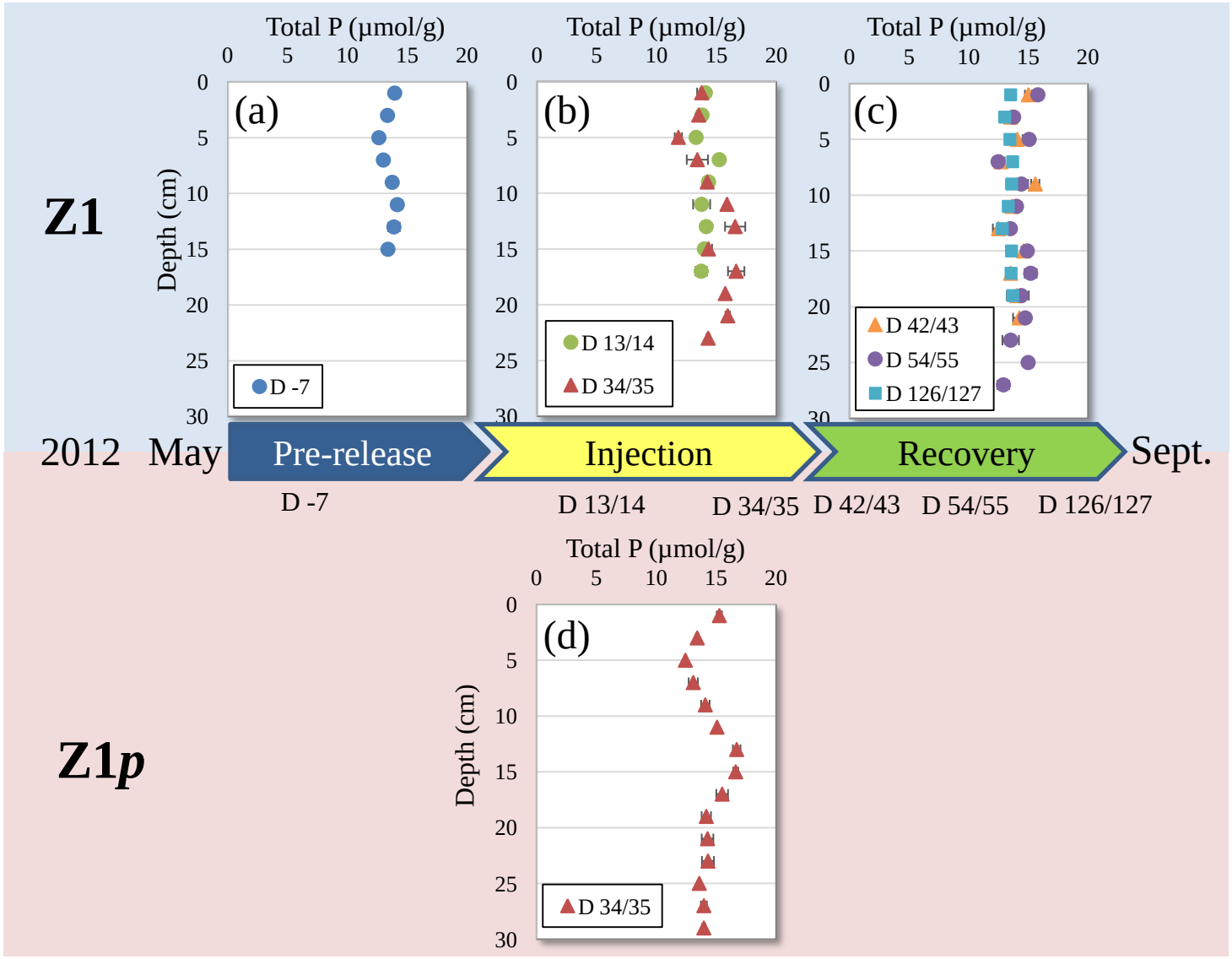

Figure3

Figure 3 (on the web only)

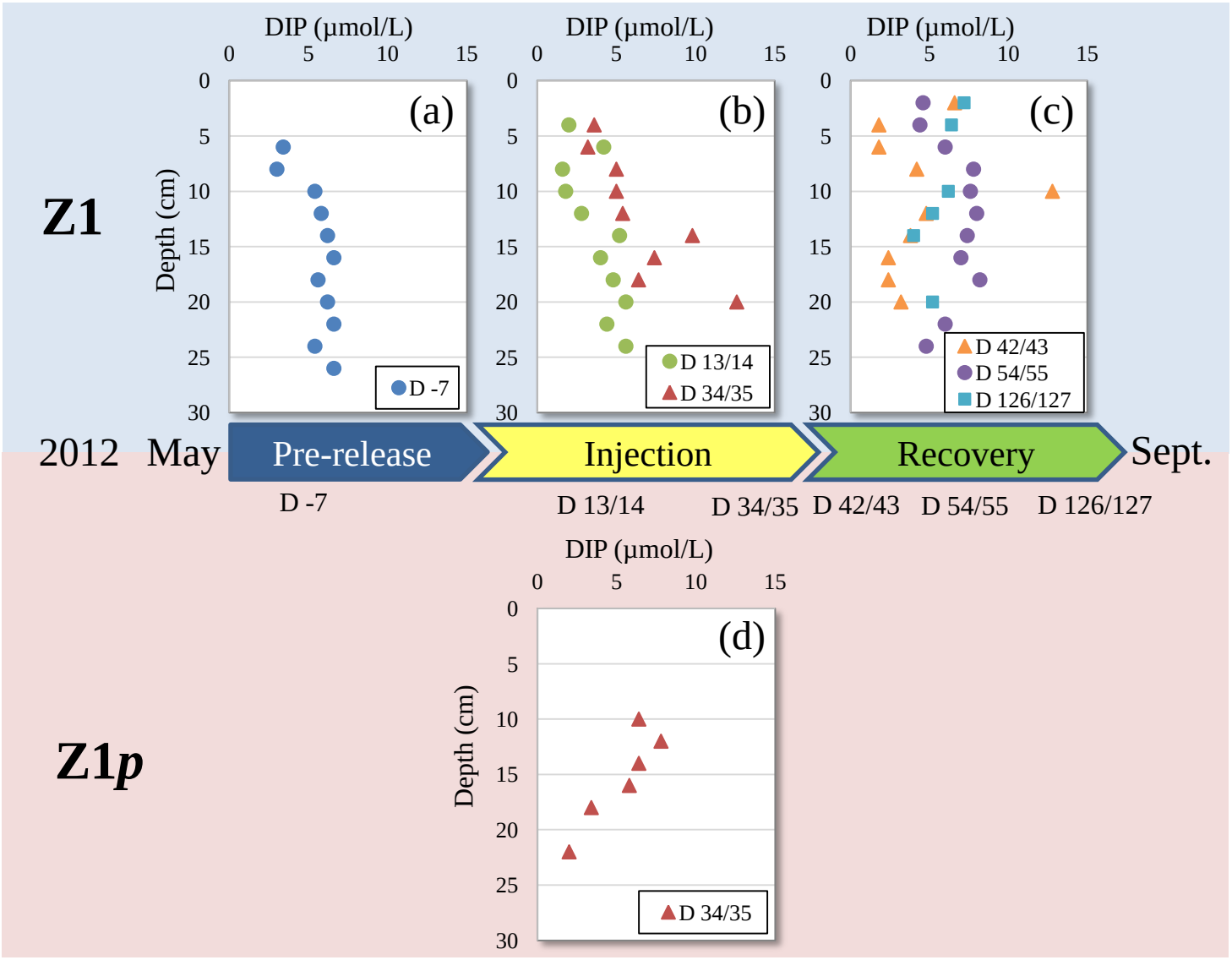

Figure 4 (on the web only)

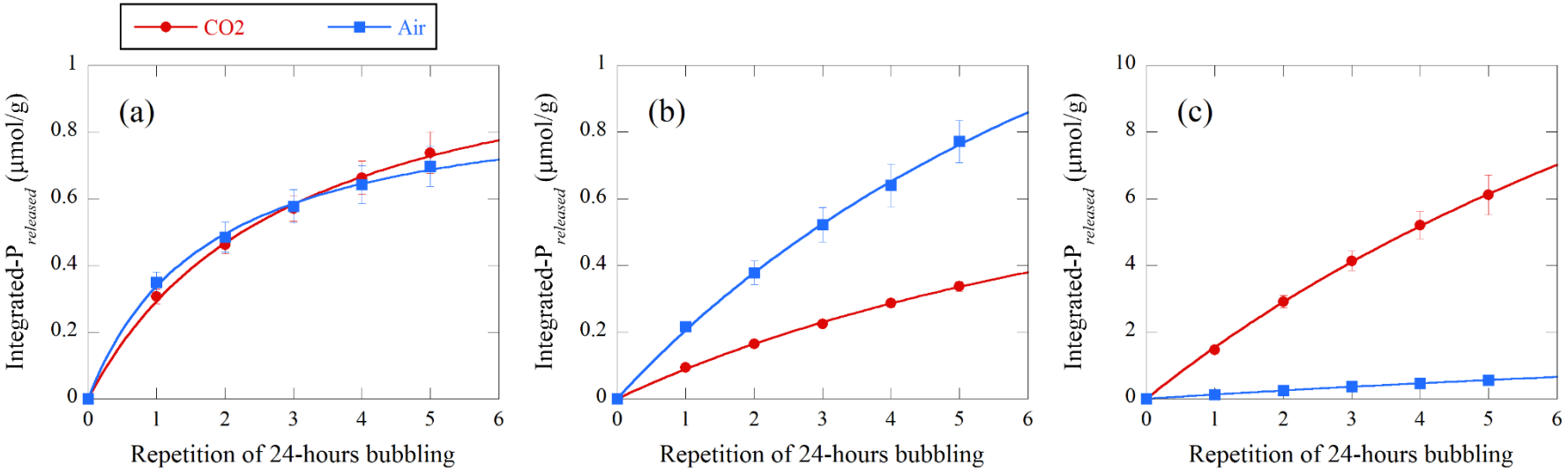

Figure5

Figure 5 (on the web only)

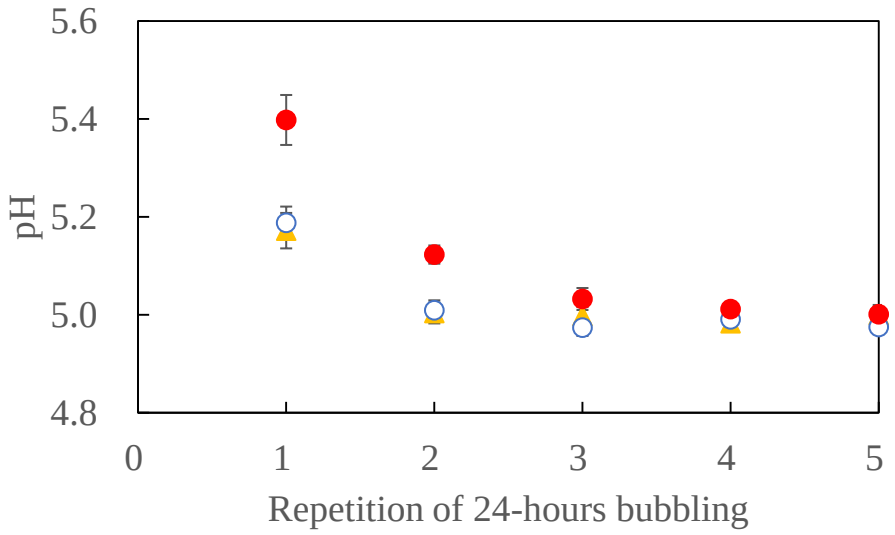

Figure6

Figure 6 (on the web only)